



Published in final edited form as:

J Mol Cell Cardiol. 2010 April ; 48(4): 725–734. doi:10.1016/j.yjmcc.2009.12.014.

GLYCOLYTIC NETWORK RESTRUCTURING INTEGRAL TO THE ENERGETICS OF EMBRYONIC STEM CELL CARDIAC DIFFERENTIATION

Susan Chung, D. Kent Arrell, Randolph S. Faustino, Andre Terzic^{*}, and Petras P. Dzeja^{*}
Marriott Heart Disease Research Program, Division of Cardiovascular Diseases, Departments of Medicine, Molecular Pharmacology and Experimental Therapeutics, and Medical Genetics, Mayo Clinic College of Medicine, Rochester, MN, USA

Abstract

Decoding of the bioenergetic signature underlying embryonic stem cell cardiac differentiation has revealed a mandatory transformation of the metabolic infrastructure with prominent mitochondrial network expansion, and a distinctive switch from glycolysis to oxidative phosphorylation. Here, we demonstrate that despite reduction in total glycolytic capacity, stem cell cardiogenesis engages a significant transcriptome, proteome, as well as enzymatic and topological rearrangement in the proximal, medial, and distal modules of the glycolytic pathway. Glycolytic restructuring was manifested by a shift in hexokinase (Hk) isoforms from Hk-2 to cardiac Hk-1, with intracellular and intermyofibrillar localization mapping mitochondrial network arrangement. Moreover, upregulation of cardiac specific enolase 3, phosphofructokinase, phosphoglucomutase and a marked increase in glyceraldehyde 3-phosphate dehydrogenase (GAPDH) phosphotransfer activity, along with apparent post-translational modifications of GAPDH and phosphoglycerate kinase, were all distinctive for derived cardiomyocytes compared to the embryonic stem cell source. Lactate dehydrogenase (LDH) isoforms evolved towards LDH-2 and LDH-3, containing higher proportions of heart-specific subunits, and pyruvate dehydrogenase isoforms rearranged between E1 α and E1 β , transitions favorable for substrate oxidation in mitochondria. Concomitantly, transcript levels of fetal pyruvate kinase isoform M2, aldolase 3 and transketolase, which shunt the glycolytic with pentose phosphate pathways, were reduced. Collectively, changes in glycolytic pathway modules indicate active redeployment which would facilitate connectivity of the expanding mitochondrial network with ATP utilization sites. Thus, the delineated developmental dynamics of the glycolytic phosphotransfer network is integral to the remodeling of cellular energetic infrastructure underlying stem cell cardiogenesis.

Keywords

bioenergetics; cardiogenesis; embryonic stem cells; proteomics; transcriptome

Robust developmental transitions in the bioenergetic system highlights embryonic stem (ES) cell differentiation into the energy-demanding cardiac phenotype, characterized by a switch

*Correspondence at Mayo Clinic, 200 First Street SW, Stabile 5, Rochester, MN 55905, USA. dzeja.petras@mayo.edu; terzic.andre@mayo.edu.

Publisher's Disclaimer: This is a PDF file of an unedited manuscript that has been accepted for publication. As a service to our customers we are providing this early version of the manuscript. The manuscript will undergo copyediting, typesetting, and review of the resulting proof before it is published in its final citable form. Please note that during the production process errors may be discovered which could affect the content, and all legal disclaimers that apply to the journal pertain.

from glycolytic to oxidative energy metabolism with expansion and maturation of the mitochondrial network [1–3]. Extensive restructuring of the metabolic transcriptome, underlying cardiogenic differentiation, involves an increased mitochondrial abundance and oxygen consumption with modified copy number of regulators of mitochondrial fusion and fission promoting mitochondrial patterning across cellular compartments [1,2,4–6]. Evolution of the mitochondrial system is paralleled by initiation of electrical activity, and by the buildup of contractile machinery requiring abundant energy supply and synchronization of excitation-contraction coupling [1,7–9].

Coordination between increased cellular energy demand and supply is secured through integrated energetic and metabolic signaling circuits composed of phosphotransfer enzymes, which couple mitochondria with cytoplasmic, myofibrillar and nuclear energetic events [10–13]. During ES cell-based cardiogenesis, developmental enhancement and restructuring of the major phosphotransfer pathway catalyzed by creatine kinase isoforms provides an energetic continuum between mitochondria and distinct cellular compartments where energy consuming processes reside [8]. Energetic rewiring is further supported by increased expression and abundance of the anchoring protein FHL2, which positions phosphotransfer enzymes to myofibrillar sites of ATP consumption [8,14,15]. While these findings implicate a comprehensive remodeling of cellular energetics during stem cell cardiac differentiation, rearrangements within the global energetic network are only partially understood.

In particular, glycolytic/glycogenolytic enzymes display an ability to provide a network capacity for transferring and distributing high-energy phosphoryls [10,13,16–18]. In the adult myocardium, the spatial arrangement of glycolytic/glycogenolytic pathway components extends from mitochondria to cellular ATPases offering a robust phosphotransfer capacity [13,19]. This property renders glycolysis a partner in the cellular energy distribution network alongside more traditional phosphotransfer pathways catalyzed by creatine and adenylate kinases [12,13,20,21]. Although the significance of glycolytic pathway components have been probed during embryonic development and cell differentiation [22–27], the evolution of the entire glycolytic network during stem cell cardiogenesis has not been determined.

Accordingly, the aim of this study was to assess the contribution and restructuring of the glycolytic phosphotransfer network during ES cell cardiac differentiation. Compared to the pluripotent source, transcriptomic and proteomic analysis revealed significant changes in transcript and protein levels in derived cardiac progeny with molecular alterations consistent with post-translational modifications of glycolytic enzymes. Immunocytochemistry and enzymatic measurements further suggested that the traditional linear, ATP-producing, glycolytic pathway transformed into a network to facilitate intracellular transfer and distribution of high-energy phosphoryls. Thus, development of the glycolytic network promotes integration of the mitochondria-based cell energetic machinery with ATP consuming processes in support of stem cell cardiogenesis.

METHODS

Stem cell differentiation

CGR8 murine ES cells were differentiated using hanging drop method [1,28]. Forming embryoid bodies were resuspended in differentiation medium, allowed to grow in suspension, and plated [1,8]. Cardiomyocytes, isolated from embryoid bodies following separation by Percoll gradient centrifugation, were cultured on gelatin coated polystyrene dishes or poly-L-lysine coated glass slides [1].

Western blotting and enzyme assays

Whole cell protein extracts were prepared by homogenization in 150 mM NaCl, 5 mM EDTA, 60 mM TRIZMA Base, 0.2% Triton X-100 and protease inhibitor cocktail (Complete Mini, EDTA-Free, Roche Applied Science). Protein concentration was determined using a detergent compatible Protein Assay kit (Bio-Rad, Hercules, CA, USA). A portion of extracts was separated by SDS-PAGE and transferred to PVDF membranes for Western blotting with specific antibodies. GAPDH activity was measured using enzymatic assay at 340 nm in (in mM unless otherwise specified): 0.1 EDTA, 2 MgCl₂, 0.2 NADH, 1 ATP, 5 3-P-Glycerate, 33 μM rotenone, 50 imidazole, pH 7.6 with 10 U/mL PGK. PGK activity was measured by modifying the previous assay, replacing PGK with 10 U/mL GAPDH. Hexokinase activity was measured at 340 nm in (in mM): 2 MgCl₂, 2 glucose, 0.2 NADP⁺, 0.4 ATP, 2.5 U/mL glucose-6-phosphate dehydrogenase and 50 imidazole, pH 7.6. LDH activity was measured using a Lactate Dehydrogenase-SL kit (Diagnostic Chemicals Limited, Oxford, CT, USA). Measurements were made by a Beckman DU 7400 spectrophotometer. Activities of LDH isoforms were assayed using a 0.8% agarose gel to separate isoforms, and the Hydragel 7 ISO-LDH kit (Sebia, Norcross, GA, USA) to detect activity. The glycolytic capacity of ES cells and ES-derived cardiomyocytes was determined by measuring lactate production rate in uncoupled (2,4-dinitrophenol, DNP, 50 μM) and uncoupled-respiration inhibited (DNP/KCN, 50 μM and 0.5 mM, respectively) states using lactate assay kit (BioVision, Mountain View, CA, USA).

Confocal microscopy

For imaging plasma and mitochondrial membrane potential, cells were incubated with 1.3 μM RH 237 (Invitrogen) and/or 0.5 μM JC-1 (Invitrogen), and washed with PBS [1,8]. Alternatively, cells were incubated with 3 μM MitoTracker Red CMH₂XRos (Invitrogen) and fixed in 3% paraformaldehyde. Cells were stained with one or more of the following antibodies: anti-Hk-1, anti-cardiac α-actinin (Santa Cruz Biotechnologies, Santa Cruz, CA, USA), and the nuclear probe 4'6-diamidino-2-phenylindole-2HCl (DAPI, Invitrogen). Fluorescent images were obtained on an LSM 510 Laser Scanning System (Carl Zeiss, Thornwood, NY, USA).

Two-dimensional gel electrophoresis and image analysis

Adherent ES cells and derived cardiomyocytes were washed repeatedly with PBS, and lysed by addition of isoelectric focusing (IEF) rehydration buffer (7 M urea, 2 M thiourea, 2% [w/v] CHAPS, 50 mM DTT). Protein extracts (n=3 biological replicates for each cell type) were quantified in triplicate by Bio-Rad protein assay, and 250 μg aliquots were added to IEF rehydration buffer containing pH 3–10 ampholytes (Bio-Rad) for resolution by immobilized pH gradient (IPG) two-dimensional gel electrophoresis. Samples were actively rehydrated in 170 mm pH 3–10 IPG Ready StripsTM (Bio-Rad) and resolved for 60 kVh, and were then reduced and alkylated prior to resolving orthogonally by 12.5% SDS-PAGE [29–32]. Gels were silver-stained, digitized at 400 dpi on a GS-800 densitometry scanner (Bio-Rad), and analyzed using PDQuest (Bio-Rad) v.7.4.0. Spot intensities were normalized by total density of individual gel images, for comparison of matching protein spots from ES cells and derived cardiomyocytes.

Protein identification by nanoelectrospray linear ion trap tandem mass spectrometry

Protein species of interest were isolated, destained, and prepared for LC-MS/MS by reduction, alkylation, tryptic digestion, peptide extraction, and drying, prior to LC-MS/MS [29,31,32]. Extracted peptides were reconstituted in 0.15% formic acid, 0.05% TFA, trap injected onto a 75 mm × 5 cm ProteoPep C18 PicoFritTM nanoflow column (New Objective, Woburn, MA, USA) in solvent A (1% acetonitrile, 0.2% formic acid in water), and eluted with increasing concentrations of solvent B (80% acetonitrile, 5% isopropanol, 0.2% formic acid in water)

using a splitless Eksigent nanoHPLC system (MDS Sciex) coupled to an LTQ mass spectrometer (ThermoElectron, Waltham, MA, USA). Continuous scanning for eluting peptide ions was carried out between 400–1400 m/z, automatically switching to MS/MS mode on ions exceeding an intensity of 1000. Raw data were converted to .dta files using Bioworks 3.2 (ThermoElectron), and merged files matching +1, 2 or 3 peptide charge states were correlated to theoretical tryptic fragments in Swiss-Prot (v.53.0, indexed 2007-05-29, comprising 269,293 sequences) using Mascot™ v.2.1. Searches were conducted on all species, with up to 2 missed cleavages, and mass tolerances of ± 2.0 Da for precursor ions and ± 0.8 Da for MS/MS product ions, allowing for the following modifications: protein N-terminal acetylation, methionine oxidation and cysteine carbamidomethylation.

Metabolic gene profiling

Total RNA isolated from ES cells or cardiomyocytes was screened using the mouse genome 430 2.0 array (Affymetrix, Inc., Santa Clara, CA, USA). Expression profiles were analyzed with the bioinformatics software suite Genespring GX 7.3 (Silicon Genetics/Agilent Technologies, Redwood City, CA, USA). Gene lists were quality filtered to remove genes with expression levels below background, and limited to report genes that changed by 1.5-fold or greater during cardiac differentiation [33].

Statistics

Comparisons between groups were performed by two-tailed Student's *t*-tests. Data are presented as mean \pm SEM; *n* refers to sample size. $P < 0.05$ was considered significant.

RESULTS

Mitochondrial abundance, glycolytic capacity and transcriptomic restructuring of glycolytic pathway

Murine stem cell differentiation into embryoid bodies represents an *in vitro* model to study developmental bioenergetics, especially during early stages of heart tissue formation [1]. Here, stem cell cardiogenesis and development of beating area was assessed by tracking the mitochondrial membrane potential sensitive probe JC-1 and the cell membrane potential sensitive probe RH 237 by confocal microscopy. Cardiomyocytes exhibited increased mitochondrial abundance (JC-1, green) and higher cell membrane potentials (RH 237, red) than the surrounding non-cardiac embryoid body (Fig. 1A). Early stage formation and maturation of cardiac beating areas, starting from a few nascent cardiomyocytes to organized structures, was followed overtime. Expansion of the mitochondrial network and integration with electrical and functional activities that take place in developing cardiomyocytes requires coordinated energy supply lines [1]. To determine glycolytic contribution, the lactate generating capacity of ES cells and derived cardiomyocytes was measured in cells uncoupled by DNP in the absence and presence of the mitochondrial respiration inhibitor KCN (Fig. 1B). Lactate production rate in both ES cells and ES-derived cardiomyocytes was higher with simultaneous uncoupling (DNP) and respiratory chain inhibition (KCN), unveiling full glycolytic potential through prevention of lactate oxidation. Notably, the total glycolytic capacity of ES-derived cardiomyocytes was markedly reduced compared to ES cells in uncoupled and uncoupled/respiration-inhibited states, by 54% and 50%, respectively ($n=4-6$, $P < 0.001$), consistent with the shift to oxidative metabolism, a more efficient means of ATP production. Microarray analysis further determined that altered glycolytic capacity was associated with changes in gene expression. Significant rearrangement of glycolytic enzyme transcripts was observed during the developmental transition from the pluripotent to the cardiomyocyte phenotype (Fig. 1C). Glycolytic genes upregulated in ES-derived cardiomyocytes included cardiac muscle-specific enolase 3 (Eno3), up ~7-fold from 0.99 ± 0.03 in ES cells to 6.70 ± 0.24 units in cardiomyocytes; hexokinase 1 (Hk1), up ~4-fold from 0.99

± 0.05 to 3.79 ± 0.6 units; phosphofructokinase (Pfk_m), up ~2-fold from 1.04 ± 0.04 to 1.90 ± 0.12 units; and phosphoglucomutase 2 (Pgm2), up ~3-fold from 1.00 ± 0.09 to 3.34 ± 0.07 units ($n=3$, $P<0.001$), respectively. Cardiomyocytes also showed upregulation of pyruvate dehydrogenase E1 α (Pdha-1), involved in oxidation of glycolysis-derived pyruvate, up 2-fold from 1.01 ± 0.05 to 2.03 ± 0.06 ($n=3$, $P<0.001$). Downregulated glycolysis transcripts included aldolase 3, down ~3-fold from 0.97 ± 0.07 to 0.38 ± 0.02 ($n=3$, $P<0.001$), and to lesser extents hexokinase 2 (Hk2), transketolase (Tkt), fetal pyruvate kinase (Pkm2) and muscle lactate dehydrogenase (Ldh1) (Fig. 1C).

Transcriptomic and topological restructuring of the proximal glycolytic pathway

Entry into the glycolytic phosphotransfer relay originates with hexokinase-catalyzed transfer of ATP phosphoryls to glucose. As the initial glycolytic step, hexokinase activity typically occurs close to or at the mitochondrial outer membrane, diverting high-energy ATP phosphoryls to specific energy consuming sites [13]. ES cell cardiac differentiation was characterized by significant upregulation of *Hk-1* (see above) and downregulation of *Hk-2* transcripts (Fig. 2A) from 0.97 ± 0.06 to 0.4 ± 0.02 ($n=3$, $P<0.001$). Total hexokinase activity on average was lower in ES-derived cardiomyocytes, 0.39 ± 0.11 versus 0.60 ± 0.14 $\mu\text{mol}/\text{min}/\text{mg}$ protein in ES cells ($n=3$). Immunocytochemistry demonstrated that, compared to ES cells (Fig. 2B, left), ES-derived cardiomyocytes have a markedly increased Hk-1 protein abundance with higher perinuclear presence and punctate accumulations intercalating with myofibrils (cardiac α -actinin, red), corresponding to mitochondrial network arrangement (Fig. 2B, right). Confocal analysis localized the majority of Hk-1 between myofibrils (Fig. 2C), where major ATP producing mitochondrial organelles reside. Other upregulated transcripts of proximal glycolytic enzymes included muscle phosphofructokinase, which accepts mitochondrial high-energy phosphoryls and feeds them into the glycolytic phosphotransfer network, and phosphoglucomutase 2, which diverts high-energy phosphoryls to the glycogenolytic network, whereas brain-type aldolase 3 (or aldolase C) was significantly downregulated (Fig. 1C). Hexokinase isoform shift and intracellular distribution, combined with phosphofructokinase and phosphoglucomutase upregulation, indicate an association of proximal glycolytic and glycogenolytic pathways with mitochondrial energy metabolism [13].

Restructuring of the medial glycolytic pathway

The middle part of the glycolytic pathway is characterized by robust phosphotransfer activity, especially in the GAPDH/PGK couple, which exceeds overall glycolytic pathway capacity [19]. Here, developmental restructuring resulted in a significant increase in GAPDH phosphotransfer activity, without an increase in either mRNA expression or total protein abundance (Fig. 3A, left). GAPDH activity increased from 0.42 ± 0.07 to 0.76 ± 0.12 $\mu\text{mol}/\text{min}/\text{mg}$ protein ($n=3$, $P<0.05$). This increase in GAPDH activity took place despite reduction in total glycolytic capacity measured by lactate production, which was decreased from 0.58 ± 0.04 in ES cells to 0.29 ± 0.02 $\mu\text{mol}/\text{min}/\text{mg}$ protein ($n=4-6$, $P<0.001$) in derived cardiomyocytes (Fig. 1B). Despite absence of change in overall protein abundance, as measured by immunoblotting and 2-D gel densitometry/mass spectrometry (Fig. S1 and Fig. 3A, upper middle/right, and lower right "Total" spot intensity), 2-D resolution of the seven identified GAPDH isoforms revealed modest increases in the five most acidic post-translationally modified forms in derived cardiomyocytes *versus* ES cells (Fig. 3A, lower right). While only a single one of these forms (spot #5) differed significantly between cell lines, the summed intensity of all modified forms (spots #1 through 6) was significantly increased in derived cardiomyocytes ($P<0.05$), with a concomitant, albeit not significant ($P=0.0622$) decrease in abundance of the unmodified form (Fig. 3A, right panels). Such pH shifts are consistent with protein post-translational modification, although the nature of the specific modifications (e.g., phosphorylation, deamidation, nitrosylation, carbamylation, etc.) has not been identified. Phosphoglycerate kinase, the other member of the GAPDH/PGK couple, and another

glycolytic phosphotransfer enzyme involved in ATP production, was downregulated in both mRNA expression (0.98 ± 0.04 to 0.88 ± 0.02) and activity (0.55 ± 0.12 to 0.35 ± 0.06 $\mu\text{mol}/\text{min}/\text{mg}$ protein, $n=3$) during ES cell cardiac differentiation (Fig. 3B, left panels). Protein expression, on the other hand, was significantly upregulated; however, the entire increase in PGK-1 abundance in ES cell-derived cardiomyocytes was accounted for by a significant increase in apparently post-translationally modified forms of the protein, without change in the abundance of unmodified PGK-1 (Fig. S1 and Fig. 3B, right panels). A number of phosphorylation sites have been reported for PGK-1 [34], although no phosphorylation sites were confirmed here.

Restructuring of the distal glycolytic pathway

Enzymes at the end of the glycolytic pathway directly provide ATP to energy consuming processes and supply mitochondria with oxidizable substrates [13,26]. Significant restructuring at the end of the glycolytic pathway also occurred during ES cell cardiogenesis, including shifts in LDH and PDH isoform expression and downregulation of fetal pyruvate kinase and transketolase transcripts. LDH isoforms shifted towards higher levels of cardiac LDH-2 and LDH-3 isoform activity at the expense of LDH-5, as demonstrated by zymogram analysis and densitometry (Fig. 4A). With total LDH activity comprising the sum of bands in each lane, LDH-2 contributed $7.32\pm 0.34\%$ to total LDH activity in ES-derived cardiomyocytes (not detected in ES cells), whereas LDH-3 contributed $16.94\pm 1.04\%$ in cardiomyocytes, more than double the $7.38\pm 1.87\%$ measured for ES cells. LDH-5 activity, on the other hand, was reduced from $63.11\pm 5.33\%$ of total activity in ES cells to $42.64\pm 1.12\%$ in cardiomyocytes (Fig. 4A). LDH-4, meanwhile, was not significantly altered, with approximately equal contributions to both ES and cardiomyocyte LDH activity ($29.5\pm 3.4\%$ versus $33.1\pm 0.3\%$). These changes were accompanied by a modest upregulation of LDH-H mRNA levels (Fig. 4B) and total LDH activity in ES cell-derived cardiomyocytes (Fig. 4C). Proteomic analysis indicated that the LDH-M subunit was post-translationally modified, with the modified form present in significantly greater abundance in cardiomyocytes than ES cells (Fig. S1 and Fig. 4D). The only known modifications to this protein are tyrosine phosphorylation and amino-terminal acetylation [35,36]. Pyruvate dehydrogenase, which functions in glycolysis-derived pyruvate oxidation, was also modified. PDH E1 α isoform mRNA levels were upregulated, while PDH E1 β levels were downregulated in ES-derived cardiomyocytes (Fig. S1 and Fig. 5A). However, proteomic analysis of 2D gel spots indicate a significant alteration in cardiomyocytes compared to ES cells, with increased abundance of PDH E1 β (Fig. 5A). Finally, pyruvate kinase, at the absolute distal end of the glycolytic pathway, was also altered during ES cell cardiogenesis, with fetal PK-m2 transcripts downregulated from ES cell mRNA levels of 0.98 ± 0.07 , to 0.67 ± 0.03 in derived cardiomyocytes (Fig. 5B). Moreover, transketolase Tkt, which connects the glycolytic and pentose phosphate pathways, also demonstrated reduced mRNA levels (from 0.99 ± 0.03 to 0.47 ± 0.01 , $n=3$, $P<0.001$) (Fig. 5C).

DISCUSSION

Cardiac differentiation and the emergence of electrical and contractile activity within nascent cardiomyocytes require adequate energy supply, and coordination in developing myofibrillar and mitochondrial networks [1,7,37]. In ES cell cardiogenesis, expansion of the mitochondrial network is paralleled by the restructuring of the major phosphotransfer pathway catalyzed by creatine kinase isoforms, providing a high-energy phosphoryl relay necessary in coupling mitochondria with ATP-consuming processes [1,8,15,21]. Here, we demonstrate transcriptome, proteome, enzymatic and topological restructuring of the glycolytic pathway during stem cell cardiogenesis. Such glycolysis-wide developmental remodeling establishes previously unrecognized metabolic circuits between the expanding mitochondria and ATP

utilization sites within the new energetic environment required for the execution of cardiogenesis.

Embryonic stem cells have a primitive architecture, high nuclear:cytosolic volume ratio and sparse mitochondria; they rely on glycolytic metabolism to meet energy needs [1,6,37,38]. Early stages of formation and maturation of cardiac beating areas organize around a core represented by the highest electrical and mitochondrial activities requiring intense energetic signaling and synchronization. The glycolytic pathway is uniquely used to provide energy support for specific cellular functions, such as maintenance of membrane ionic gradients and electrical activity and could provide a link between mitochondria and cellular ATP-consuming processes [13,39]. Specifically, ES cell cardiogenesis was associated with a shift in hexokinase isoforms from Hxk-2 towards Hxk-1, which associates with cardiac mitochondria [40,41] and serves as a point for high-energy phosphoryl groups to enter the glycolytic phosphotransfer network [13]. Indeed, cardiomyocytes had higher Hxk-1 protein content with a dappled pattern of intracellular localization corresponding to mitochondrial network arrangement throughout the cell and specifically in the intermyofibrillar space. This data is in line with the demonstration that Hxk-1 is localized mainly in the heart at early stages of embryonic development [23]. Although adult cardiomyocytes display both Hxk-1 and Hxk-2 isoforms, Hxk-2 is predominant [40]. Under physiological conditions, Hxk-2 is mainly localized in the cytosol, whereas Hxk-1 is largely bound to mitochondria [41]. Translocation of hexokinase to the mitochondria increases its kinetic efficiency and decreases its susceptibility to product inhibition [41]. It also decreases free radical formation in the mitochondria and prevent apoptosis [42–44]. Leukemia inhibitory factor, LIF, which maintains ES cells in an undifferentiated state, increases Hxk-2 association with mitochondria and protects against oxidant or Ca^{2+} -stimulated permeability transition-pore opening [45]. Insulin is a major factor regulating hexokinase binding to mitochondria and slows down the decline in stem cell numbers and function that normally occurs with age [40,46]. Thus, isoform composition and intracellular positioning of hexokinase provides a target towards increased stem cell survival and differentiation into specific cell lineage.

A significant increase in GAPDH phosphotransfer activity in ES cell-derived cardiomyocytes and apparent post-translational modification of GAPDH and PGK1 in both cell populations takes place as here detected by proteomic analysis. The augmentation in GAPDH activity occurred despite reduced total glycolytic capacity as measured by lactate production. In this regard, in addition to measurements of total glycolytic capacity of ES cells and derived cardiomyocytes, assessment of glycolytic flux would provide further insight in glycolysis-catalyzed energetic dynamics. The increase in GAPDH activity could be attributed to a shift in isoform composition as a result of post-translational modifications, alternative splicing or transcription of different genes [27]. All three mechanisms contribute to the diversity of GAPDH which manifests in multiple intracellular localizations, including the membrane, cytosol and nucleus [47,48]. A variety of GAPDH post-translational modifications have been identified, including auto-ADP-ribosylation, glutathionylation, S-nitrosylation, threonine and tyrosine phosphorylation, active site oxidation and carbonylation [49–51]. Most of these modifications typically result in enzyme inhibition, yet here there was a substantial increase in GAPDH activity in nascent cardiomyocytes. GAPDH phosphorylation, in general, has a positive impact on catalytic activity [50–52]. Predictions for multiple GAPDH phosphorylation sites [53] are consistent with the observed mass and pI of unmodified and modified GAPDH protein spots shown here. However, the modest difference in extent of post-translational modification between ES and ES-derived cardiomyocytes is unlikely to account for the difference in activity, unless it can be demonstrated that the modifications accounting for pI shifts in ES cells differ from those giving rise to pI shifts in ES-derived cardiomyocytes. During embryonic development, cytosolic GAPDH is engaged in a metabolic feedback loop with glucose and pyruvate found in the culture medium, thereby affecting ATP levels and ATP-

dependent chromatin remodeling that allows activation of specific genes [54]. In addition, GAPDH isoforms have distinct roles with respect to apoptosis and both the activities and isoforms are differentially regulated during apoptosis and cell differentiation [47,50]. The data presented here indicate that GAPDH rearrangements are induced by stem cell cardiogenesis to meet increasing energetic and metabolic signaling requirements.

PGK1, one of two isoforms of phosphoglycerate kinase and an active glycolytic phosphotransfer enzyme involved in phosphoryl exchange and ATP generation [13,26], was downregulated in both mRNA expression and activity during ES cell cardiac differentiation. Protein expression, however, was upregulated with significant increases in post-translationally modified forms of the protein. A recent study indicates that the P_{gk1} promoter is highly active in cardiac beating areas of embryoid bodies [55]. The metabolic significance of rearrangements in PGK, which works in tandem with the GAPDH in catalyzing high-energy phosphoryl transfer, is not fully understood. These data exemplify the intricate regulation at transcriptional, translational and post-translational levels of glycolytic enzymes to match new energetic challenges of the developing cardiac tissue.

Functioning as a highly adaptable metabolic intermediate transfer system, LDH isoforms govern lactate-pyruvate conversion and substrate supply to mitochondria. Here with cardiac differentiation, LDH isoforms shifted towards LDH2 and LDH3 composed of muscle and heart subunits. The kinetic characteristics of LDH heart (H) subunits foster function in aerobic environment to facilitate lactate to pyruvate conversion [56,57]. Mixed H and M subunit containing isoforms (LDH2, LDH3) catalyze the lactate-pyruvate equilibrium reaction and could translate changes in the substrate balance throughout cellular compartments [13,58]. Thus, the biological logic of such transformations in the glycolytic pathway apparently lies in discharging ATP and supplying substrates to mitochondria necessary for maintenance of newly-derived cell energetic competence.

Significant rearrangements took place in mitochondrial enzyme pyruvate dehydrogenase, PDH, which provides a link between glycolysis and the Krebs cycle facilitating pyruvate oxidation and substrate supply to the extended mitochondrial network [24,57,59]. As an energetic enzyme, PDH exhibits critical significance in embryonic development [24]. During ES cell cardiogenesis the PDH complex was affected at the mRNA level by upregulation of the E1 α subunit, downregulation of the E1 β subunit, and an increase in the E1 β protein. Such rearrangements in PDH together with changes in LDH system are favorable for substrate supply and oxidation in mitochondria. Since PDH dynamics typically follow mitochondrial respiration rate which is increased in cardiac differentiation [1], it is conceivable that PDH activity will be higher in ES cell-derived cardiomyocytes although measurements of PDH activity will be required to further assess the relationship between oxidative phosphorylation and glycolysis in cardiogenesis.

Among downregulated glycolysis transcripts during ES cell cardiogenesis were aldolase 3, transketolase (Tkt) and fetal pyruvate kinase (Pkm2). While downregulation of aldolase 3 and Pkm2 indicates shift in isoform composition and intracellular distribution of corresponding catalytic modules, the decrease in Tkt suggests uncoupling of glycolysis from the biosynthetic pentose phosphate pathway. Such alterations could promote an energy distribution function of the glycolytic network [10,13]. Pyruvate kinase catalyzes the distal ATP-delivery step of the glycolytic pathway and is usually localized close to ATP consumption sites [13,26]. During differentiation from the fetus to the adult the M2-type disappears while the M1-type becomes predominant in heart and skeletal muscle [60,61]. Thus, the observed downregulation of Pkm2 transcripts during stem cell cardiogenesis is consistent with previous reports indicating an isoform shift in this glycolytic enzyme.

Glucose and glycolysis are critical for substrate supply and energy provision in many cell types even in those that rely on aerobic metabolism [13,56,58,62]. Spatial extension of the glycolytic pathway (Fig. 6) indicate that it can comprise a network of phosphotransfer circuits and metabolite shuttles, which facilitates high-energy phosphoryl delivery, lactate/pyruvate and Pi shuttling and, thus, maintain cellular energy and redox balance [10,13,26]. High-energy phosphoryls from ATP, used to phosphorylate glucose and fructose-6-phosphate at the mitochondrial site traverse the glycolytic pathway, and in turn can be used to rephosphorylate ADP through the pyruvate kinase-catalyzed reaction at remote ATP utilization sites. Additional phosphoryls can be transferred through the near-equilibrium GAPDH/PGK couple catalyzing robust phosphoryl exchange [13,19]. Glycolytic rearrangements during stem cell cardiogenesis takes place in clusters of hexokinase/phosphoglucose isomerase (Hex/PGI/PGM), phosphofructokinase/aldolase/triosephosphate isomerase (PFK/Aldo/TPI/TKT), glyceraldehyde-3-phosphate dehydrogenase/phosphoglycerate kinase (GAPDH/PGK) and phosphoglycerate mutase/enolase/pyruvate kinase (PGM/ENO/PK), where spatially directed phosphoryl transfer could occur through bidirectional substrate exchange enzymatic chains (Fig. 6). With stem cell cardiogenesis significant changes occurred in the LDH system which through sequentially arranged LDH-catalyzed reactions can facilitate transfer of pyruvate and NADH from remote cellular sites where pyruvate kinase resides towards mitochondria [13, 58]. And finally, reorganization of the PDH complex is favorable for integration of glycolytic network with mitochondrial energy metabolism (Fig. 6). Thus, in this network mode of glycolytic arrangement high energy phosphoryls picked up from mitochondria or generated by glycolysis can be preferentially delivered and used to support specific cellular functions, such as maintenance of membrane ionic gradients, cell motility, muscle contraction and nuclear processes which are critical for stem cell cardiogenesis [1,7–9,38].

In summary, this study uncovers molecular and cellular mechanisms that are used during stem cell cardiac differentiation to support the emerging energetic infrastructure of nascent cardiomyocytes and to adapt gene expression programs to the metabolic context. The delineated wide range transcriptomic, proteomic, post-translational, enzymatic and topological restructuring of the glycolytic pathway indicates that during ES cell cardiogenesis it assumes a new energetic function of facilitating substrate supply and transferring high-energy phosphoryls from mitochondria to ATP utilization sites. Such developmental enhancement and restructuring of the glycolytic network provide an energetic continuum between mitochondria and other cellular compartments that integrates processes necessary for stem cell cardiogenesis.

Supplementary Material

Refer to Web version on PubMed Central for supplementary material.

Acknowledgments

This work was supported by grants from the National Institutes of Health HL 85744 (P.D.) and HL083439 (A.T.), Marriott Heart Disease Research Program, Marriott Foundation, Ted Nash Long Life Foundation and Ralph Wilson Medical Research Foundation. A.T. holds the Mayo Clinic Marriott Family Professorship in Cardiovascular Research.

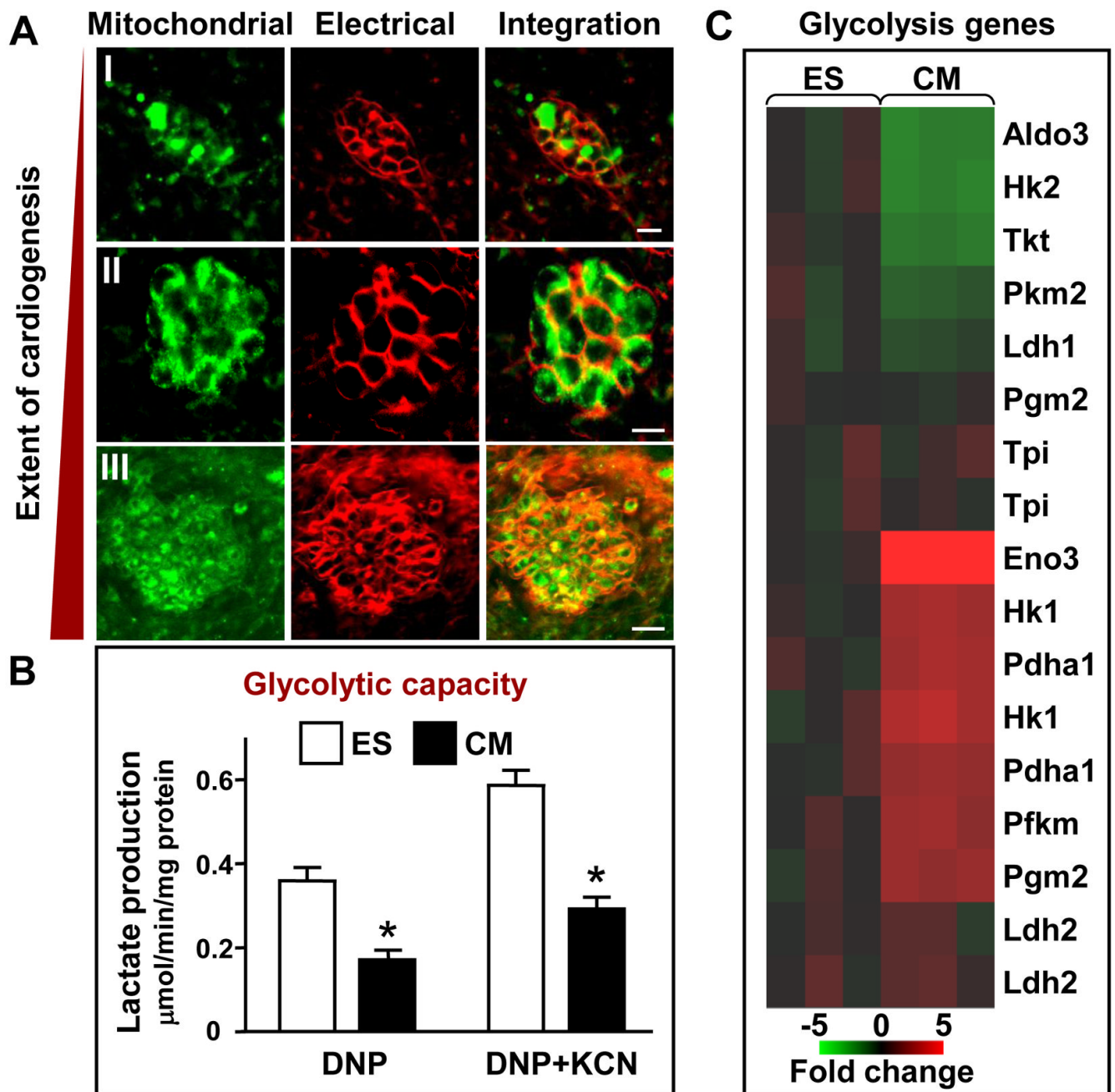
References

1. Chung S, Dzeja PP, Faustino RS, Perez-Terzic C, Behfar A, Terzic A. Mitochondrial oxidative metabolism is required for the cardiac differentiation of stem cells. *Nat Clin Pract Cardiovasc Med* 2007;4 (Suppl 1):S60–7. [PubMed: 17230217]
2. Facucho-Oliveira JM, Alderson J, Spikings EC, Egginton S, St John JC. Mitochondrial DNA replication during differentiation of murine embryonic stem cells. *J Cell Sci* 2007;120:4025–34. [PubMed: 17971411]

3. St John JC, Ramalho-Santos J, Gray HL, Petrosko P, Rawe VY, Navara CS, et al. The expression of mitochondrial DNA transcription factors during early cardiomyocyte in vitro differentiation from human embryonic stem cells. *Cloning Stem Cells* 2005;7:141–53. [PubMed: 16176124]
4. Niethammer P, Kueh HY, Mitchison TJ. Spatial patterning of metabolism by mitochondria, oxygen, and energy sinks in a model cytoplasm. *Curr Biol* 2008;18:586–91. [PubMed: 18406136]
5. Scarpulla RC. Nuclear control of respiratory chain expression by nuclear respiratory factors and PGC-1-related coactivator. *Ann N Y Acad Sci* 2008;1147:321–34. [PubMed: 19076454]
6. Spitzkovsky D, Sasse P, Kolossov E, Bottinger C, Fleischmann BK, Hescheler J, et al. Activity of complex III of the mitochondrial electron transport chain is essential for early heart muscle cell differentiation. *Faseb J* 2004;18:1300–2. [PubMed: 15180963]
7. Behfar A, Faustino RS, Arrell DK, Dzeja PP, Perez-Terzic C, Terzic A. Guided stem cell cardiopoiesis: discovery and translation. *J Mol Cell Cardiol* 2008;45:523–9. [PubMed: 18835562]
8. Chung S, Dzeja PP, Faustino RS, Terzic A. Developmental restructuring of the creatine kinase system integrates mitochondrial energetics with stem cell cardiogenesis. *Ann N Y Acad Sci* 2008;1147:254–63. [PubMed: 19076447]
9. Nelson TJ, Faustino RS, Chiriach A, Crespo-Diaz R, Behfar A, Terzic A. CXCR4+/FLK-1+ biomarkers select a cardiopoietic lineage from embryonic stem cells. *Stem Cells* 2008;26:1464–73. [PubMed: 18369102]
10. Dzeja PP, Terzic A. Phosphotransfer networks and cellular energetics. *J Exp Biol* 2003;206:2039–47. [PubMed: 12756286]
11. Ingwall JS. Transgenesis and cardiac energetics: new insights into cardiac metabolism. *J Mol Cell Cardiol* 2004;37:613–23. [PubMed: 15350834]
12. Saks V, Dzeja P, Schlattner U, Vendelin M, Terzic A, Wallimann T. Cardiac system bioenergetics: metabolic basis of the Frank-Starling law. *J Physiol* 2006;571:253–73. [PubMed: 16410283]
13. Dzeja, P.; Chung, S.; Terzic, A. Integration of adenylate kinase, glycolytic and glycogenolytic circuits in cellular energetics. In: Saks, V., editor. *Molecular System Bioenergetics: Energy for Life*. Weinheim, Germany: Wiley-VCH; 2007. p. 265-301.
14. Lange S, Auerbach D, McLoughlin P, Perriard E, Schafer BW, Perriard JC, et al. Subcellular targeting of metabolic enzymes to titin in heart muscle may be mediated by DRAL/FHL-2. *J Cell Sci* 2002;115:4925–36. [PubMed: 12432079]
15. Wallimann T, Wyss M, Brdiczka D, Nicolay K, Eppenberger HM. Intracellular compartmentation, structure and function of creatine kinase isoenzymes in tissues with high and fluctuating energy demands: the 'phosphocreatine circuit' for cellular energy homeostasis. *Biochem J* 1992;281 (Pt 1): 21–40. [PubMed: 1731757]
16. de Groof AJ, Oerlemans FT, Jost CR, Wieringa B. Changes in glycolytic network and mitochondrial design in creatine kinase-deficient muscles. *Muscle Nerve* 2001;24:1188–96. [PubMed: 11494272]
17. Dzeja PP, Terzic A, Wieringa B. Phosphotransfer dynamics in skeletal muscle from creatine kinase gene-deleted mice. *Mol Cell Biochem* 2004;256–257:13–27.
18. Dzeja PP, Zeleznikar RJ, Goldberg ND. Adenylate kinase: kinetic behavior in intact cells indicates it is integral to multiple cellular processes. *Mol Cell Biochem* 1998;184:169–82. [PubMed: 9746320]
19. Kingsley-Hickman PB, Sako EY, Mohanakrishnan P, Robitaille PM, From AH, Foker JE, et al. 31P NMR studies of ATP synthesis and hydrolysis kinetics in the intact myocardium. *Biochemistry* 1987;26:7501–10. [PubMed: 3427090]
20. Dzeja PP, Bast P, Pucar D, Wieringa B, Terzic A. Defective metabolic signaling in adenylate kinase AK1 gene knock-out hearts compromises post-ischemic coronary reflow. *J Biol Chem* 2007;282:31366–72. [PubMed: 17704060]
21. Saks V, Kaambre T, Guzun R, Anmann T, Sikk P, Schlattner U, et al. The creatine kinase phosphotransfer network: thermodynamic and kinetic considerations, the impact of the mitochondrial outer membrane and modelling approaches. *Subcell Biochem* 2007;46:27–65. [PubMed: 18652071]
22. Aguiari P, Leo S, Zavan B, Vindigni V, Rimessi A, Bianchi K, et al. High glucose induces adipogenic differentiation of muscle-derived stem cells. *Proc Natl Acad Sci U S A* 2008;105:1226–31. [PubMed: 18212116]
23. Fritz HL, Smoak IW, Branch S. Hexokinase I expression and activity in embryonic mouse heart during early and late organogenesis. *Histochem Cell Biol* 1999;112:359–65. [PubMed: 10603075]

24. Johnson MT, Mahmood S, Hyatt SL, Yang HS, Soloway PD, Hanson RW, et al. Inactivation of the murine pyruvate dehydrogenase (Pdha1) gene and its effect on early embryonic development. *Mol Genet Metab* 2001;74:293–302. [PubMed: 11708858]
25. Kondoh H, Leonart ME, Nakashima Y, Yokode M, Tanaka M, Bernard D, et al. A high glycolytic flux supports the proliferative potential of murine embryonic stem cells. *Antioxid Redox Signal* 2007;9:293–9. [PubMed: 17184172]
26. Masters C. Cellular differentiation and the microcompartmentation of glycolysis. *Mech Ageing Dev* 1991;61:11–22. [PubMed: 1779698]
27. Sun XH, Tso JY, Lis J, Wu R. Differential regulation of the two glyceraldehyde-3-phosphate dehydrogenase genes during *Drosophila* development. *Mol Cell Biol* 1988;8:5200–5. [PubMed: 3149711]
28. Behfar A, Zingman LV, Hodgson DM, Rauzier JM, Kane GC, Terzic A, et al. Stem cell differentiation requires a paracrine pathway in the heart. *Faseb J* 2002;16:1558–66. [PubMed: 12374778]
29. Arrell DK, Niederlander NJ, Faustino RS, Behfar A, Terzic A. Cardioinductive network guiding stem cell differentiation revealed by proteomic cartography of tumor necrosis factor alpha-primed endodermal secretome. *Stem Cells* 2008;26:387–400. [PubMed: 17991915]
30. Zlatkovic J, Arrell DK, Kane GC, Miki T, Seino S, Terzic A. Proteomic profiling of KATP channel-deficient hypertensive heart maps risk for maladaptive cardiomyopathic outcome. *Proteomics* 2009;9:1314–25. [PubMed: 19253285]
31. Arrell DK, Niederlander NJ, Perez-Terzic C, Chung S, Behfar A, Terzic A. Pharmacoproteomics: advancing the efficacy and safety of regenerative therapeutics. *Clin Pharmacol Ther* 2007;82:316–9. [PubMed: 17671447]
32. Behfar A, Perez-Terzic C, Faustino RS, Arrell DK, Hodgson DM, Yamada S, et al. Cardiopoietic programming of embryonic stem cells for tumor-free heart repair. *J Exp Med* 2007;204:405–20. [PubMed: 17283208]
33. Faustino RS, Behfar A, Perez-Terzic C, Terzic A. Genomic chart guiding embryonic stem cell cardiopoiesis. *Genome Biol* 2008;9:R6. [PubMed: 18184438]
34. Sweet SM, Bailey CM, Cunningham DL, Heath JK, Cooper HJ. Large scale localization of protein phosphorylation by use of electron capture dissociation mass spectrometry. *Mol Cell Proteomics* 2009;8:904–12. [PubMed: 19131326]
35. Cooper JA, Esch FS, Taylor SS, Hunter T. Phosphorylation sites in enolase and lactate dehydrogenase utilized by tyrosine protein kinases in vivo and in vitro. *J Biol Chem* 1984;259:7835–41. [PubMed: 6330085]
36. Stegink LD, Vestling CS. Rat liver lactate dehydrogenase. Amino-terminal and acetylation status. *J Biol Chem* 1966;241:4923–30. [PubMed: 5925863]
37. Van Blerkom J. Mitochondria as regulatory forces in oocytes, preimplantation embryos and stem cells. *Reprod Biomed Online* 2008;16:553–69. [PubMed: 18413065]
38. Perez-Terzic C, Faustino RS, Boorsma BJ, Arrell DK, Niederlander NJ, Behfar A, et al. Stem cells transform into a cardiac phenotype with remodeling of the nuclear transport machinery. *Nat Clin Pract Cardiovasc Med* 2007;4 (Suppl 1):S68–76. [PubMed: 17230218]
39. Dhar-Chowdhury P, Malester B, Rajacic P, Coetzee WA. The regulation of ion channels and transporters by glycolytically derived ATP. *Cell Mol Life Sci* 2007;64:3069–83. [PubMed: 17882378]
40. Southworth R, Davey KA, Warley A, Garlick PB. A reevaluation of the roles of hexokinase I and II in the heart. *Am J Physiol Heart Circ Physiol* 2007;292:H378–86. [PubMed: 16951044]
41. Wilson JE. Isozymes of mammalian hexokinase: structure, subcellular localization and metabolic function. *J Exp Biol* 2003;206:2049–57. [PubMed: 12756287]
42. Abu-Hamad S, Zaid H, Israelson A, Nahon E, Shoshan-Barmatz V. Hexokinase-I protection against apoptotic cell death is mediated via interaction with the voltage-dependent anion channel-1: mapping the site of binding. *J Biol Chem* 2008;283:13482–90. [PubMed: 18308720]
43. Anflous-Pharayra K, Cai ZJ, Craigen WJ. VDAC1 serves as a mitochondrial binding site for hexokinase in oxidative muscles. *Biochim Biophys Acta* 2007;1767:136–42. [PubMed: 17207767]
44. Gerbitz KD, Gempel K, Brdiczka D. Mitochondria and diabetes. Genetic, biochemical, and clinical implications of the cellular energy circuit. *Diabetes* 1996;45:113–26. [PubMed: 8549853]

45. Miyamoto S, Murphy AN, Brown JH. Akt mediates mitochondrial protection in cardiomyocytes through phosphorylation of mitochondrial hexokinase-II. *Cell Death Differ* 2008;15:521–9. [PubMed: 18064042]
46. Hsu HJ, Drummond-Barbosa D. Insulin levels control female germline stem cell maintenance via the niche in *Drosophila*. *Proc Natl Acad Sci U S A* 2009;106:1117–21. [PubMed: 19136634]
47. Chuang DM, Hough C, Senatorov VV. Glyceraldehyde-3-phosphate dehydrogenase, apoptosis, and neurodegenerative diseases. *Annu Rev Pharmacol Toxicol* 2005;45:269–90. [PubMed: 15822178]
48. Hara MR, Snyder SH. Nitric oxide-GAPDH-Siah: a novel cell death cascade. *Cell Mol Neurobiol* 2006;26:527–38. [PubMed: 16633896]
49. Lind C, Gerdes R, Schuppe-Koistinen I, Cotgreave IA. Studies on the mechanism of oxidative modification of human glyceraldehyde-3-phosphate dehydrogenase by glutathione: catalysis by glutaredoxin. *Biochem Biophys Res Commun* 1998;247:481–6. [PubMed: 9642155]
50. Sirover MA. New insights into an old protein: the functional diversity of mammalian glyceraldehyde-3-phosphate dehydrogenase. *Biochim Biophys Acta* 1999;1432:159–84. [PubMed: 10407139]
51. Villen J, Beausoleil SA, Gerber SA, Gygi SP. Large-scale phosphorylation analysis of mouse liver. *Proc Natl Acad Sci U S A* 2007;104:1488–93. [PubMed: 17242355]
52. Tisdale EJ. Glyceraldehyde-3-phosphate dehydrogenase is phosphorylated by protein kinase C α and plays a role in microtubule dynamics in the early secretory pathway. *J Biol Chem* 2002;277:3334–41. [PubMed: 11724794]
53. Obenauer JC, Cantley LC, Yaffe MB. Scansite 2.0: Proteome-wide prediction of cell signaling interactions using short sequence motifs. *Nucleic Acids Res* 2003;31:3635–41. [PubMed: 12824383]
54. Boiani M, Scholer HR. Regulatory networks in embryo-derived pluripotent stem cells. *Nat Rev Mol Cell Biol* 2005;6:872–84. [PubMed: 16227977]
55. Wang R, Liang J, Jiang H, Qin LJ, Yang HT. Promoter-dependent EGFP expression during embryonic stem cell propagation and differentiation. *Stem Cells Dev* 2008;17:279–89. [PubMed: 18447643]
56. Fantin VR, St-Pierre J, Leder P. Attenuation of LDH-A expression uncovers a link between glycolysis, mitochondrial physiology, and tumor maintenance. *Cancer Cell* 2006;9:425–34. [PubMed: 16766262]
57. Van Hall G. Lactate as a fuel for mitochondrial respiration. *Acta Physiol Scand* 2000;168:643–56. [PubMed: 10759601]
58. Gladden LB. Lactate metabolism: a new paradigm for the third millennium. *J Physiol* 2004;558:5–30. [PubMed: 15131240]
59. Semenza GL. Oxygen-dependent regulation of mitochondrial respiration by hypoxia-inducible factor 1. *Biochem J* 2007;405:1–9. [PubMed: 17555402]
60. Imamura K, Tanaka T. Multimolecular forms of pyruvate kinase from rat and other mammalian tissues. I. Electrophoretic studies. *J Biochem* 1972;71:1043–51. [PubMed: 4342282]
61. Yamada K, Noguchi T. Nutrient and hormonal regulation of pyruvate kinase gene expression. *Biochem J* 1999;337 (Pt 1):1–11. [PubMed: 9854017]
62. Jones RG, Thompson CB. Tumor suppressors and cell metabolism: a recipe for cancer growth. *Genes Dev* 2009;23:537–48. [PubMed: 19270154]



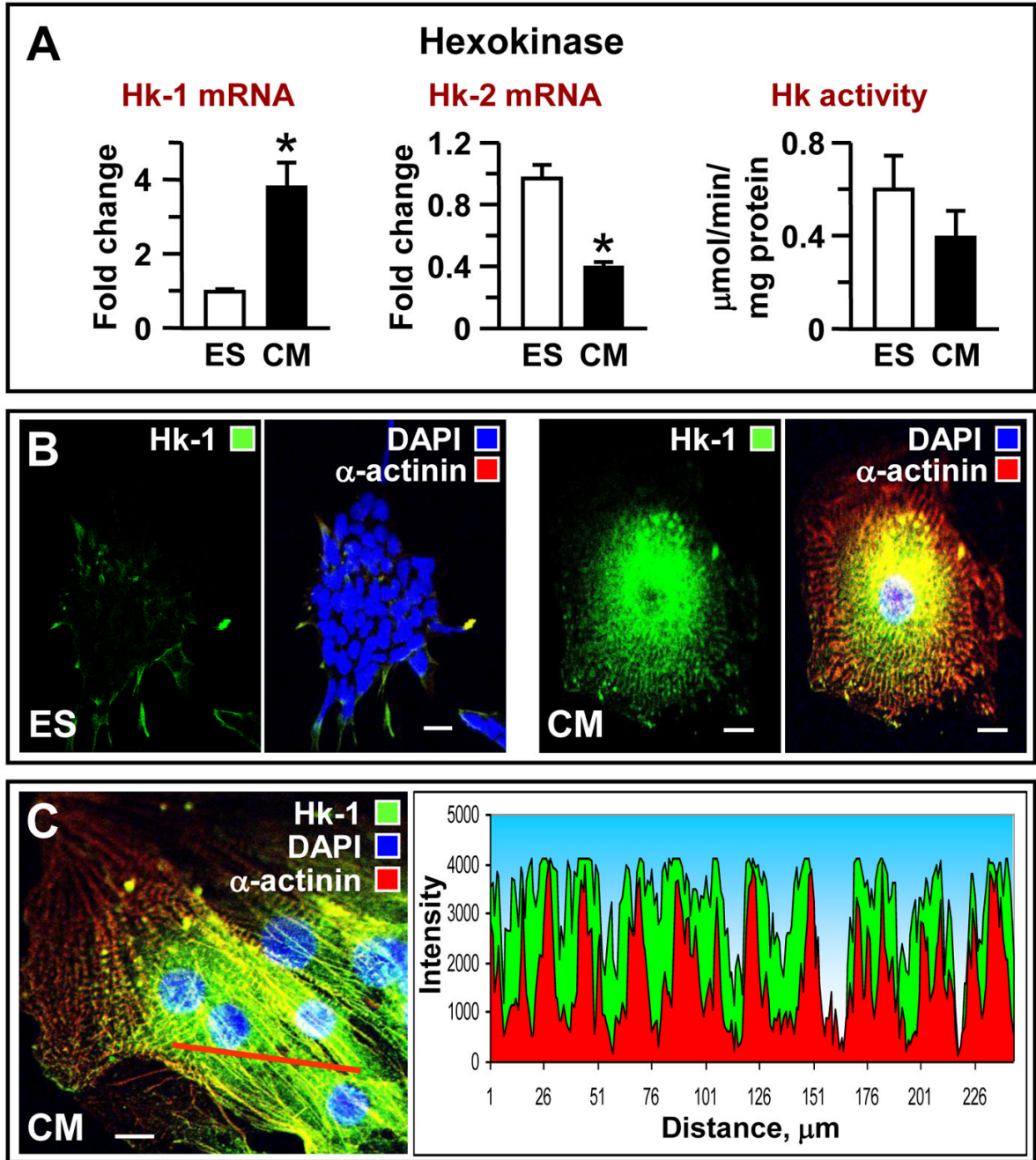


Figure 2. Transcriptomic and topological restructuring of the entry step in the glycolytic pathway: increase connection with mitochondria

(A) A shift in hexokinase isoforms from Hxk-2 towards Hxk-1 and marginal reduction in enzyme activity in ES cell-derived cardiomyocytes (CM). Immunocytochemistry indicates that, compared to (B) ES cells, (C) cardiomyocytes have increased Hxk-1 abundance with a stippled pattern of intracellular localization and higher perinuclear concentration corresponding to mitochondrial network arrangement; the myofibrillar mesh is stained with α -actinin (red). Scale bar indicates 10 μm .

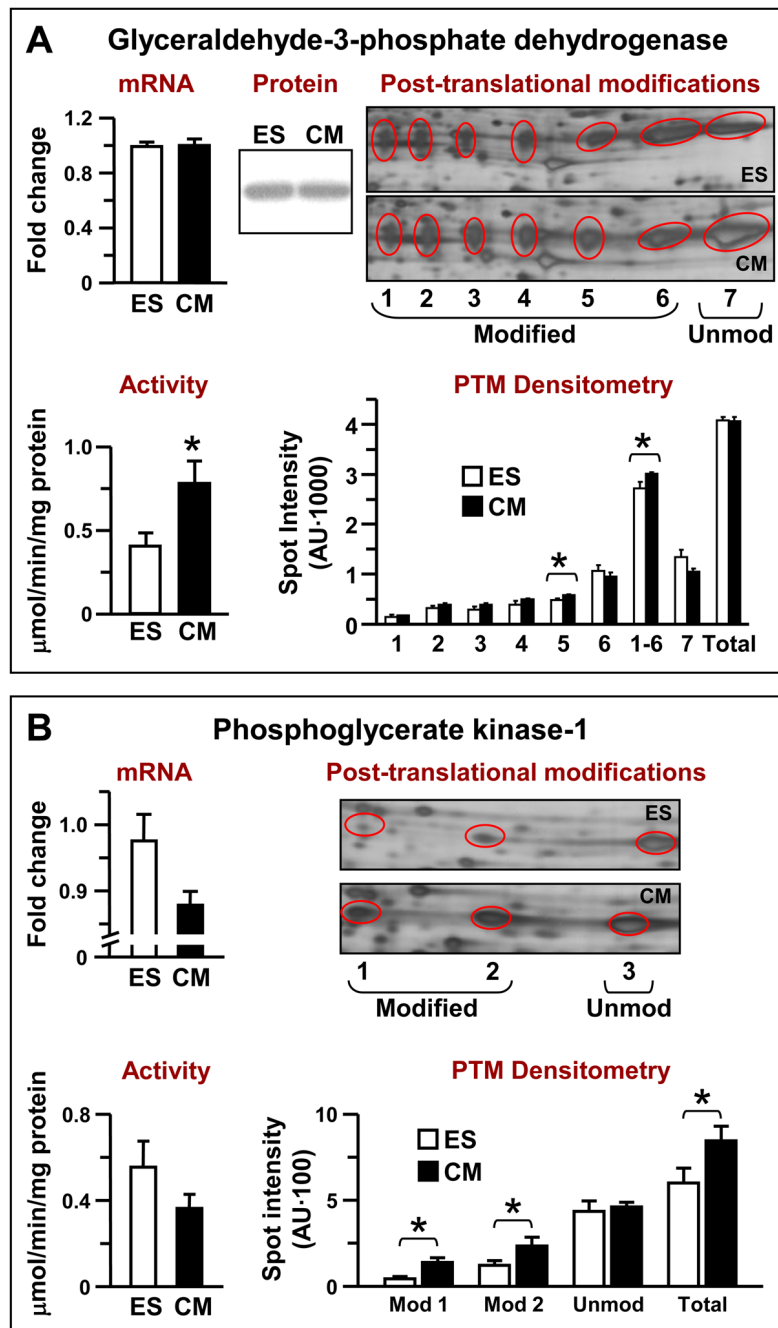


Figure 3. Transcriptomic, proteomic and enzymatic restructuring of the middle segment of the glycolytic pathway

(A) Embryonic stem (ES) cell cardiac differentiation is associated with increased GAPDH phosphotransfer activity, without parallel mRNA or protein changes, although there is a modest increase in post-translational modification of GAPDH in ES cell-derived cardiomyocytes (CM) detected by 2-D gels, densitometry and MS/MS analysis. (B) Downregulation of messenger RNA levels of PGK1 and total PGK activity with increased post-translational modifications of protein detected by 2-D gels, densitometry and MS/MS analysis during ES cell cardiac differentiation.

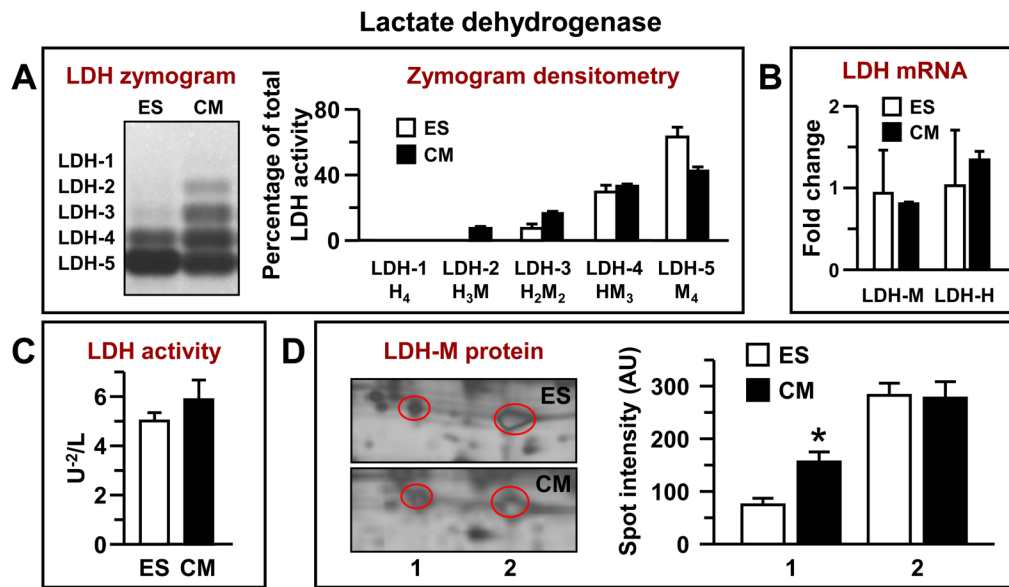


Figure 4. Transcriptomic, proteomic and enzymatic restructuring of the ending segment of the glycolytic pathway
 (A) Zymogram (left) analysis by densitometry (right) indicates a shift in LDH isoforms towards cardiac LDH-2 and LDH-3 in ES cell-derived cardiomyocytes. (B) LDH mRNA levels and (C) activity in ES cells and cardiomyocytes. (D) Proteomic analysis of LDH-M in ES cells and cardiomyocytes.

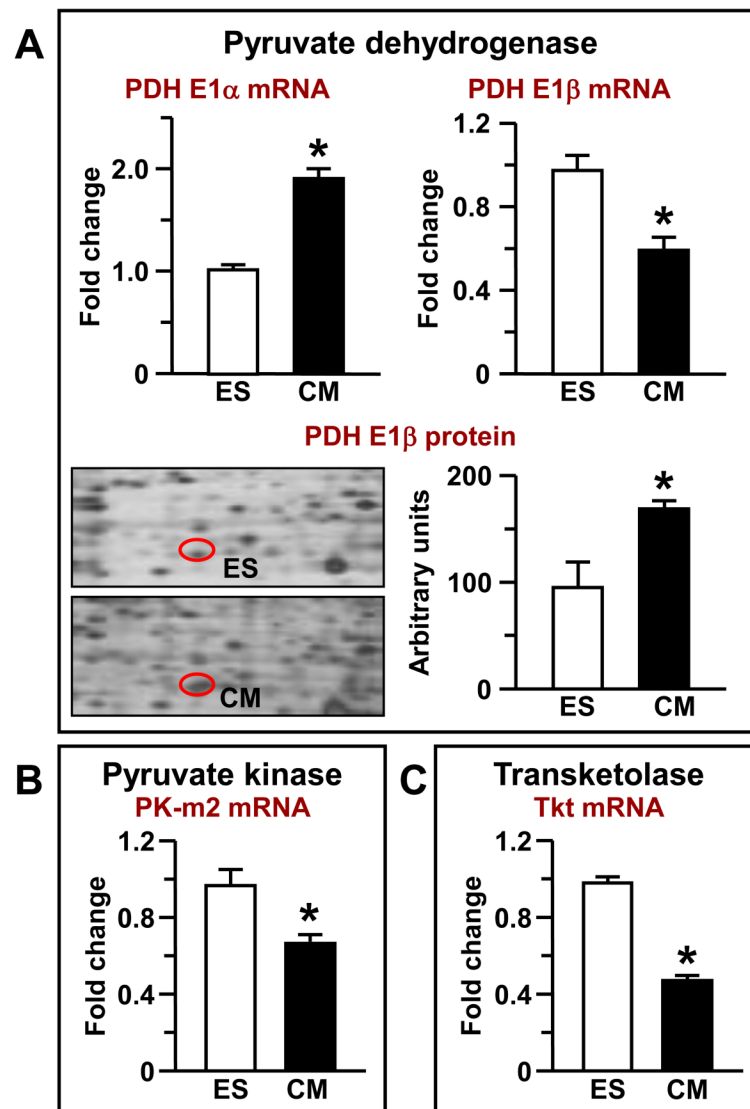


Figure 5. A shift in pyruvate dehydrogenase (PDH) isoforms and downregulation of fetal pyruvate kinase PK-m2 and transketolase Tkt transcripts during ES cell cardiac differentiation (A and B) Differential regulation of PDH isoform transcriptome and proteome during ES cell cardiogenesis. (C) Reduced fetal PK-m2 and (B) Tkt transcript levels in ES cell-derived cardiomyocytes.

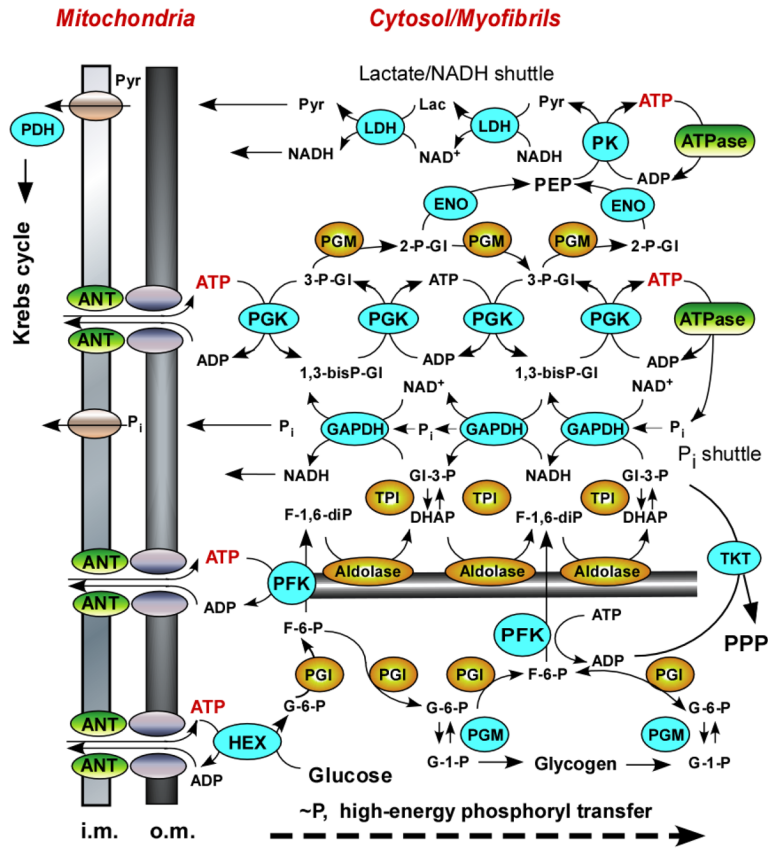


Figure 6. Developmental restructuring and intracellular positioning of glycolytic phosphotransfer enzymes facilitate integration of mitochondrial energetics with ATP utilization sites
 Schematic representation of the glycolytic pathway transformed into a network to assume a new energetic function of high-energy phosphotransfer from mitochondria to cellular ATPases. Marked in cyan color are components undergoing transcriptome, proteome or enzymatic activity restructuring during stem cell cardiogenesis. PPP – pentose phosphate pathway; ANT – adenine nucleotide translocator; i.m. and o.m. – inner and outer mitochondrial membranes, respectively.